Theoretical Study of the Reaction Mechanism and Role of Water Clusters in the Gas-Phase Hydrolysis of $SiCl_4$

Stanislav K. Ignatov*,†
University of Nizhny Novgorod, 23 Gagarin Avenue, Nizhny Novgorod 603600, Russia

Petr G. Sennikov‡
Institute of High-Pure Substances of RAS, Nizhny Novgorod 603600, Russia

Alexey G. Razuvaev§
Chemistry Institute of Nizhny Novgorod State University, Nizhny Novgorod 603600, Russia

Lev A. Chuprov||
Institute of High-Pure Substances of RAS, Nizhny Novgorod 603600, Russia

Otto Schrems⊥
Alfred-Wegener Institut für Polar- und Meeresforschung, Bremerhaven, Germany

Bruce S. Ault#
University of Cincinnati, Cincinnati, Ohio 45221

Received: March 11, 2003; In Final Form: July 17, 2003

The energies and thermodynamic parameters of the elementary reactions involved in the gas-phase hydrolysis of silicon tetrachloride were studied using ab initio quantum chemical methods (up to MP4//MP2/6-311G-(2d,2p)), density functional (B3LYP/6-311++G(2d,2p)), and G2(MP2) theories. The proposed mechanism of hydrolysis consists of the formation of $SiCl_{4-x}(OH)_x$ ($x = 1-4$), disiloxanes $Cl_{4-x}(OH)_{x-1}Si-O-SiCl_{4-x}(OH)_{x-1}$, chainlike and cyclic siloxane polymers $[-SiCl_2-O-]_n$, dichlorosilanone $Cl_2Si=O$, and silicic acid $(HO)_2Si=O$. Thermodynamic parameters were estimated, and the transition states were located for all of the elementary reactions. It was demonstrated that the experimentally observed kinetic features for the high-temperature hydrolysis are well described by a regular bimolecular reaction occurring through a four-membered cyclic transition state. In contrast, the low-temperature hydrolysis reaction cannot be described by the traditionally accepted bimolecular pathway for Si−Cl bond hydrolysis because of high activation barrier (E_a = 107.0 kJ/mol, $\Delta G^{\ddagger}$ = 142.5 kJ/mol) nor by reactions occurring through three- or four-molecular transition states proposed earlier for reactions occurring in aqueous solution. The transition states of $SiCl_4$ with one- and two-coordinated water molecules were located; these significantly decrease the free energy of activation $\Delta G^{\ddagger}$ (to 121.3 and 111.5 kJ/mol, correspondingly). However, this decrease in $\Delta G^{\ddagger}$ is not sufficient to account for the high value of the hydrolysis rate observed experimentally under low-temperature conditions.

Introduction

The hydrolysis of $SiCl_4$ is a potential source of impurities in many modern technologies that rely on the fabrication of high-purity materials for fiber optics and SiO_2 coverage, specifically where the material properties are determined by the number of point defects (e.g., extrinsic OH groups).[1] Because the number of defects is largely determined by the kinetics of the physicochemical processes occurring in the hydrolytic mixture, it is very desirable to know the mechanism, as well as the thermodynamic and kinetic parameters of the elementary stages of this process, occurring in the gas phase at relatively low temperatures under equilibrium conditions. Although the high-temperature or plasma-chemical processes of fabrication of aerosils, silica gels, and related species from $SiCl_4$ have been studied in detail from a technological point of view,[2] the gas-phase hydrolysis mechanism itself under equilibrium conditions has only been studied in a very general way.

The commonly accepted mechanism for the hydrolysis of $SiCl_4$ can be represented by the scheme[3]

$$SiCl_4 + H_2O \rightarrow SiCl_3OH + HCl \quad \text{(primary hydrolysis)} \quad (1)$$

$$Cl_3SiOH + HOSiCl_3 \rightarrow Cl_3Si-O-SiCl_3 + H_2O \quad \text{(condensation)} \quad (2)$$

$$Cl_3Si-O-SiCl_3 + H_2O \rightarrow Cl_3Si-O-SiCl_2-OH + H_2O \quad \text{(further branching, chain growth and cyclization)} \quad (3)$$

... etc.

which takes place when the $H_2O/SiCl_4$ ratio is low. When this ratio is relatively high, then the following mechanism has been proposed:[3]

† E-mail: ignatov@ichem.unn.runnet.ru.
‡ E-mail: sen@ihps.nnov.ru.
§ E-mail: tcg@ichem.unn.runnet.ru.
|| E-mail: chuprov@ihps.nnov.ru.
⊥ E-mail: oschrems@awi-bremerhaven.de.
E-mail: ault@email.uc.edu.

10.1021/jp034618h CCC: $25.00
Published on Web 09/19/2003

$$SiCl_4 + H_2O \rightarrow SiCl_3OH + HCl \quad \text{(primary hydrolysis)} \quad (1a)$$

$$SiCl_3OH + H_2O \rightarrow SiCl_2(OH)_2 + HCl \quad (1b)$$

$$SiCl_2(OH)_2 + H_2O \rightarrow SiCl(OH)_3 + HCl \quad (1c)$$

$$SiCl(OH)_3 + H_2O \rightarrow Si(OH)_4 + HCl \quad (1d)$$

$$Si(OH)_4 + Si(OH)_4 \rightarrow Si(OH)_3{-}O{-}Si(OH)_3 \quad \text{(condensation)} \quad (2)$$

$$Si(OH)_3{-}O{-}Si(OH)_3 + Si(OH)_4 \rightarrow Si(OH)_3{-}O{-}Si(OH)_2{-}O{-}Si(OH)_3 + HCl \quad (3)$$

... etc. (further branching, chain growth and cyclization)

It is important to note that these proposed mechanisms are based primarily on measurements of pressure changes during the reaction. One conclusion from these experiments is that mixing $SiCl_4$ and H_2O in the gas phase does not result in a pressure increase up to 50 °C and, if the partial pressure of $SiCl_4$ is not greater than 300 Torr, then the gas-phase hydrolysis does not occur in the temperature range 25−100 °C in 48 h.[3] Reaction of $SiCl_4$ and water begins at a temperature of 500 °C and results in the formation of various siloxanes of growing size and, when the temperature increases, finally leads to crystalline silicon dioxide. It is frequently accepted that, at least at high temperatures, the condensation step of this scheme is very fast and the rate-limiting reaction is the Si−Cl hydrolysis step, which is considered as a regular bimolecular reaction.[3−5] For the condensation step, two different reaction channels are feasible, homofunctional (4a) and heterofunctional condensation (4b). Usually, homofunctional condensation (4a) is considered to be the more kinetically favorable process.[6]

$$SiCl_3OH + SiCl_3OH \rightarrow SiCl_3{-}O{-}SiCl_3 + H_2O \quad (4a)$$

$$SiCl_4 + SiCl_3OH \rightarrow SiCl_3{-}O{-}SiCl_3 + HCl \quad (4b)$$

Since the 1950s, several experimental results have appeared in the literature which cannot be described by the scheme (1)−(3). First, on the basis of product yield analysis of the partial $SiCl_4$ hydrolysis conducted in a liquid mixture of H_2O and $(CH_3)_2O$,[7] it was concluded that the hydrolysis passes through the formation of the termolecular intermediate complex $O(CH_3)_2 \cdot H_2O \cdot HCl$, which is much more reactive than the separate H_2O and $O(CH_3)_2$ molecules. Although this complex was not characterized by physical methods, its presence was required to describe all of the features observed in the experiment. Later, direct infrared spectroscopic analysis of impurities in liquid $SiCl_4$ was performed[8] and it was concluded that one of the major impurities of $SiCl_4$ (apart from HCl and siloxane $SiCl_3{-}O{-}SiCl_3$) were the OH-containing species. Contrary to the proposal that the condensation step is very rapid, the infrared absorptions of the OH groups were very stable and disappeared only after boiling the reaction mixture for 4 h. Simultaneously, the concentration of siloxanes increased in a 1:1 ratio relative to the concentration of the OH derivatives. This study concluded that the rate-limiting step under water-deficient conditions is the heterofunctional condensation reaction 4b and that $SiCl_3$-OH is the most thermodynamically favorable intermediate in the hydrolysis process.

In the past two decades, the development of new experimental techniques has allowed direct measurements of the gas-phase kinetics of the hydrolysis process.[9] Infrared spectrophotometry of the methylchlorosilanes $SiCl_{4-x}(CH_3)_x$ was conducted in the temperature range 20−80 °C, and the reaction orders, initial reaction rates, and temperature dependence of the rate constants were measured. Surprisingly, they found that (a) silicon tetrachloride hydrolysis takes place even at 20 °C, (b) the reaction rate shows the temperature maximum at 30−40 °C, and (c) the order of the reaction with respect to H_2O is 2, not 1 (as suggested by the commonly accepted scheme (1)−(3)). It should be noted that the observed reaction order could not be obtained by combining the equations of the scheme described above.

In a recent study,[10] these experiments were repeated on different experimental apparatus, over wider temperature ranges. This study confirmed that the low-temperature hydrolysis does take place in the range 20−100 °C and that the reaction orders are 1 and 2 for $SiCl_4$ and H_2O, correspondingly. Also, the reaction rate decreases with increasing temperature up to 100 °C, corresponding to a negative energy of activation, and goes practically to zero at 100 °C. However, at 470 °C, the hydrolysis begins again and is a first-order reaction for both $SiCl_4$ and H_2O. In the range 470−800 °C, $SiCl_4$ hydrolysis is a regular bimolecular reaction with a positive activation energy of 121.9 kJ/mol.[10]

Thus, the reaction mechanism for the hydrolysis of $SiCl_4$ given by eqs 1−3 cannot be considered as absolutely correct or, at least, complete. Equations 1−3 cannot explain the second-order dependence on water observed at low temperatures. Treating the primary hydrolysis reaction 1 as a regular, bimolecular rate-limiting step cannot explain the negative activation energy observed at low temperatures and is inconsistent with the observation that the condensation step is slow. All of these facts point to the conclusion that the complete reaction mechanism is more complicated than scheme (1)−(3) and requires additional consideration. It should also be noted that there have been no reliable estimates for the kinetic and thermodynamic parameters of the individual steps (1)−(3), which makes discussion of the reaction mechanism speculative.

Since the 1990s, there have been a number of theoretical studies of the mechanism of siloxane formation.[11−17] First, Kudo and Gordon[11,12] investigated the reactions of $SiHCl_3$ and $SiH_{4-x}(OH)_x$ with water at the Si−Cl hydrolysis step and at further condensation steps. They estimated the activation energies and found that the energy of activation at both the primary hydrolysis and activation steps can be significantly lowered by the coordination of additional water molecules to the transition structures. However, no rate constants were calculated and no direct comparison with experiment was made. Thus, the application of this mechanism to the gas-phase reaction of $SiCl_4$ remains to be elucidated. Later, Okumoto et al.[13] and Ignatyev et al.[14] demonstrated similar results for the condensation reactions of $SiH_{4-x}(OH)_x$, $SiR_{4-x}(OH)_x$ and related compounds. However, as before, the mechanism was not validated by the quantitative comparison with experimental data. Jug and Gloriozov[15,16] proposed an alternative mechanism of siloxane growth which is clearly applicable to the further stages of hydrolysis, because the breaking of the first Si−Cl bond can be considered as an initial step of this mechanism. Jug and coworkers[17] also investigated the various radical processes probably occurring during the high-temperature synthesis of SiO_2 from $SiCl_4$ and O_2. They demonstrated that radical reactions between $SiCl_4$ and O_2 in the gas phase lead to a wide variety of products but are characterized by very high activation barriers (240 kJ/mol and higher) and, therefore, are highly unlikely under the soft conditions of the room-temperature hydrolysis.

TABLE 1: Energies and Thermodynamic Parameters of Reaction 1 Calculated at Different Levels of Theory (kJ/mol)

level of theory	$\Delta_r E_{tot}$	$\Delta_r(E_{tot}+ZPE)$	$\Delta_r H°(298)$	$\Delta_r G°(298)$
MP2/6-311G(d,p)[a]	−24.6	−15.8	−16.3	−21.6
MP2/6-311G++(d,p)[a]	−9.9	−16.0	−16.2	−22.8
MP2/6-311++G(2d,2p)[a]	−16.0	−22.0	−22.5	−28.0
B3LYP/6-311G(d,p)	−41.6	−47.9	−48.3	−53.8
B3LYP/6-311G(2d,2p)	−39.2	−45.3	−45.7	−51.4
B3LYP/6-311++G(2d,2p)	−16.9	−23.2	−23.6	−29.6
B3LYP/6-311++G(3df,2p)	−19.1	−25.3	−25.6	−31.5
G2(MP2)	−10.3	−16.4	−16.8	−22.4

[a] PC GAMESS calculation with the Cartesian (6d) basis functions.

Thus, one of the probable explanations for the fast gas-phase hydrolysis reaction at low temperature is the coordination of additional water molecules to the transition structures. Although such reactions are clearly feasible in aqueous solution, the applicability of this mechanism to the gas phase must be additionally proved on the basis of available experimental data on the direct gas-phase kinetic measurements.

The main goal of the present work is to estimate theoretically the thermodynamic and kinetic parameters of the reactions constituting a possible reaction mechanism for the hydrolysis of $SiCl_4$ and, if possible, to account for the experimental observations mentioned above.

Theoretical Methods

All of the chemical structures were optimized by gradient methods implemented in the Gaussian 98[18] and PC GAMESS[19] packages at the B3LYP/6-311G(2d,2p) density functional level of theory.

The thermodynamic calculations for relatively small molecules were performed using G2(MP2) theory.[20] For siloxanes with three and more silicon atoms, when the usage of extrapolation methods was impossible, direct thermodynamic calculations were performed on the basis of geometric parameters and vibrational frequencies obtained at the B3LYP/6-311++G(2d,-2p) level in the harmonic approximation. The scale factor 0.9613 was used for the harmonic frequencies.[21] Special attention was paid to hindered rotation within the molecules under consideration. The effect of hindered rotation on the entropy and the Gibbs free energy was taken into account using the E2 procedure of East[22] and the Pitzer-Gwinn independent rotor approximation.[23] In some cases, special consideration of large-amplitude motions was also undertaken using the ADANIMEHS program[24] originally developed for PES scanning of nonrigid systems.

All the transition states were located using the procedures implemented in Gaussian 98 and characterized by frequency calculations. Standard transition state theory was used for the rate constant calculations.

Results and Discussion

Thermodynamic Considerations. It is well-known that the level of quantum chemical theory used for the calculation of thermodynamic parameters has a crucial effect on the results of thermochemical analysis. Although the best results are obtained with extrapolation methods (e.g., G2(MP2) and others), the use of these methods is often impractical for large molecules. Therefore, we used more practical procedures that provide satisfactory accuracy in the calculation of thermodynamic functions. Table 1 shows the results obtained at the MP2 and B3LYP levels of theory with various basis sets in comparison to G2(MP2) values for the energy and thermodynamic parameters of reaction 1. As is evident from the table, the energy values obtained at the B3LYP/6-311++G(2d,2p) level are close to the G2(MP2) results. Although the values of the enthalpy and Gibbs free energy are better at the MP2/6-311++G(d,p) level, the energy of reaction at this level is too low, which is the result of occasional compensation of errors in this method. Therefore, we have chosen the B3LYP/6-311++G(2d,2p) level as a practical procedure that provides a reliable estimate of the reaction energies of large molecules. For some critical results, we used MP2/6-311++G(d,p) and G2(MP2) theory with the B3LYP optimized structures as an additional method of verifying the DFT results.

Table 2 shows the thermodynamic parameters for the elementary steps of the hydrolysis of $SiCl_4$ calculated at the G2(MP2) and B3LYP/6-311++G(2d,2p) levels. On the basis of these results, one can conclude that the elementary reactions of hydrolysis are exothermic and favorable from the thermodynamic point of view (enthalpy of reaction is −15 to −17 kJ/mol and the Gibbs free energy −12 to −30 kJ/mol). This conclusion constitutes the most important difference between the hydrolysis of $SiCl_4$ the analogous system $SiF_4 + H_2O$. Earlier, we studied the gas-phase hydrolysis of silicon tetrafluoride SiF_4[25] using gas-phase FTIR spectroscopy combined with quantum chemical calculations. This study found that the primary hydrolysis reactions in this system are characterized by positive values of both the reaction enthalpy and the Gibbs free energy. This demonstrates that this reaction is controlled by thermodynamic factors, at least during the initial steps of hydrolysis. At first glance, it seems probable that another halogen compound, $SiCl_4$, should be similar to SiF_4 with respect to hydrolysis reactions. However, the calculations do not support this suggestion.

We can see also from Table 2 that successive hydrolysis of the Si−Cl bonds of $SiCl_4$ is characterized by decreasing energetic effects and the Gibbs free energy in the sequence:

$$SiCl_4 > SiCl_3OH > SiCl_2(OH)_2 > SiCl(OH)_3$$

This is not surprising taking into account that the Si−O bond is stronger than the Si−Cl bond. However, it is interesting that the process of breaking the Si−Cl bond and forming the Si−O bond is increasingly harder the more OH groups are bound to Si. This fact was already described by Wichmann[26] whereas the opposite effect was found by Schlegel[27] in the $SiCl_{4-x}H_x$ decomposition to $SiCl_{3-x}H_x$ and Cl radicals when the increase of x resulted in a weakening of Si−Cl bond.

The above sequence leads to the conclusion that the equilibrium involving disproportionation reactions of the hydroxychloro derivatives $SiCl_{4-x}(OH)_x$ should be shifted to the side of derivatives with smaller x. Table 3 shows the energies and thermodynamic parameters of the successive disproportionation reactions, leading to an increase in the number of OH groups on the silicon atom. As can be seen from the data, the most stable compound is trichlorosilanol $SiCl_3OH$ and that species should prevail in an equilibrium mixture. This conclusion is in agreement with experimental data from the infrared spectroscopy of impurities in liquid $SiCl_4$ at room temperature.[8] As mentioned above, it was shown in this study that the OH-containing impurities are slowly converted into siloxanes in a 1:1 ratio by reaction 4b, confirming that the most stable OH-containing species under water deficient conditions is $SiCl_3OH$.

Table 4 shows the calculated energies and thermodynamic parameters of the condensation reactions for the hydrolysis of $SiCl_4$. One can conclude from these data that the elementary reactions of condensation are, as a rule, less thermodynamically profitable. The heterofunctional condensation reaction is characterized by negative values of the reaction enthalpy and the

TABLE 2: Energies, Standard Enthalpies, Standard Gibbs Free Energies and the Equilibrium Constants for the Elementary Reactions of Primary $SiCl_4$ Hydrolysis Calculated at the G2(MP2) and B3LYP/6-311++G(2d,2p) (in Parentheses) Levels (kJ/mol)

elementary reaction	$\Delta_r E_{tot}$	$\Delta_r(E_{tot}+ZPE)$	$\Delta_r H°_{298}$	$\Delta_r G°_{298}$
$SiCl_4 + H_2O \rightarrow SiCl_3OH + HCl$	−10.3 (−16.9)	−16.4 (−23.2)	−16.8 (−23.6)	−22.4 (−29.6)
$SiCl_3OH + H_2O \rightarrow SiCl_2(OH)_2 + HCl$	−11.2 (−17.3)	−17.0 (−22.6)	−17.4 (−23.5)	−16.7 (−21.3)
$SiCl_2(OH)_2 + H_2O \rightarrow SiCl(OH)_3 + HCl$	−10.2 (−14.8)	−15.2 (−20.1)	−16.0 (−20.9)	−13.8 (−18.9)
$SiCl(OH)_3 + H_2O \rightarrow Si(OH)_4 + HCl$	−10.7 (−13.7)	−14.5 (−17.8)	−15.9 (−19.2)	−12.4 (−15.6)

TABLE 3: Energies, Standard Enthalpies, Standard Gibbs Free Energies and the Equilibrium Constants for the Elementary Reactions of $SiCl_{4-x}(OH)_x$ Disproportionation Calculated at the G2(MP2) and B3LYP/6-311++G(2d,2p) (in Parentheses) Levels (kJ/mol)

reaction	$\Delta_r E_{tot}$	$\Delta_r(E_{tot}+ZPE)$	$\Delta_r H°_{298}$	$\Delta_r G°_{298}$
$SiCl_3OH \rightarrow SiCl_4 + SiCl_2(OH)_2$	−0.9 (−0.4)	−0.6 (0.7)	−0.6 (0.1)	5.7 (8.3)
$SiCl_3OH + SiCl_2(OH)_2 \rightarrow SiCl_4 + SiCl(OH)_3$	0.1 (2.1)	1.2 (3.2)	0.7 (2.7)	8.6 (10.7)
$2SiCl_2(OH)_2 \rightarrow SiCl_4 + Si(OH)_4$	0.7 (5.7)	3.7 (8.0)	2.3 (7.0)	3.1 (16.4)

TABLE 4: Energies, Standard Enthalpies, and Standard Gibbs Free Energies for the Elementary Reactions of Homo- and Heterofunctional Condensation of Hydroxoderivatives $SiCl_{4-x}(OH)_x$ Calculated at the B3LYP/6-311++G(2d,2p) and G2(MP2) (in Parentheses) Levels (kJ/mol)

reaction	$\Delta_r E_{tot}$	$\Delta_r(E_{tot}+ZPE)$	$\Delta_r H°_{298}$	$\Delta_r G°_{298}$
$SiCl_3OH + SiCl_4 \rightarrow SiCl_3-O-SiCl_3 + HCl$	−17.4 (−39.4)	−26.5 (−47.9)	−22.8 (−44.0)	−24.2 (−48.6)
$2SiCl_3OH \rightarrow SiCl_3-O-SiCl_3 + H_2O$	−0.5 (−29.1)	−3.2 (−31.5)	0.7 (−27.2)	5.4 (−26.2)
$2SiCl_2(OH)_2 \rightarrow SiCl_2(OH)-O-SiCl_2(OH) + H_2O$	−2.7	−6.5	−2.2	0.0
$2SiCl(OH)_3 \rightarrow SiCl(OH)_2-O-SiCl(OH)_2 + H_2O$	−12.7	−14.7	−11.3	−5.4
$2Si(OH)_4 \rightarrow Si(OH)_3-O-Si(OH)_3 + H_2O$	−16.4	−18.7	−15.2	−10.8

TABLE 5: Summary of Reaction Energies and Thermodynamic Parameters for the proposed $SiCl_4$ Hydrolysis Mechanism (B3LYP/6-311++G(2d,2p)) (kJ/mol)

reaction	$\Delta_r E_{tot}$	$\Delta_r(E_{tot}+ZPE)$	$\Delta_r H°_{298}$	$\Delta_r G°_{298}$
Primary Hydrolysis				
$SiCl_4 + H_2O = SiCl_3OH + HCl$	−16.9	−23.2	−23.6	−29.6
$SiCl_4 + 2H_2O = SiCl_2(OH)_2 + 2HCl$	−34.2	−45.8	−47.0	−50.9
$SiCl_4 + 3H_2O = SiCl(OH)_3 + 3HCl$	−49.0	−65.9	−67.9	−69.8
$SiCl_4 + 4H_2O = Si(OH)_4 + 4HCl$	−62.7	−83.7	−87.1	−69.8
Condensation and Further Hydrolysis				
$SiCl_4 + {}^1/_2H_2O = {}^1/_2SiCl_3-O-SiCl_3 + HCl$	−17.1	−24.8	−23.2	−26.9
$SiCl_4 + {}^3/_2H_2O = {}^1/_2SiCl_2(OH)-O-SiCl_2(OH) + 2HCl$	−35.6	−49.1	−48.1	−50.9
$SiCl_4 + {}^5/_2H_2O = {}^1/_2SiCl(OH)_2-O-SiCl(OH)_2 + 3HCl$	−55.4	−73.2	−73.6	−72.5
$SiCl_4 + {}^7/_2H_2O = {}^1/_2Si(OH)_3-O-Si(OH)_3 + 4HCl$	−70.9	−93.0	−94.7	−90.8
Chainlike Polymerization				
$SiCl_4 + {}^2/_3H_2O = {}^1/_3SiCl_3(OSiCl_2)_2Cl + {}^4/_3HCl$	−24.2	−34.5	−32.2	−37.4
Cyclization				
$SiCl_4 + H_2O = {}^1/_2Si_2Cl_4O_2 + 2HCl$	28.5	12.3	13.6	−4.4
$SiCl_4 + H_2O = {}^1/_3Si_3Cl_6O_3 + 2HCl$	−31.6	−46.9	−45.3	−55.1
Formation of H_2SiO_3 and $SiCl_2O$				
$SiCl_4 + 3H_2O = SiO(OH)_2 + 4HCl$	200.2	170.2	170.3	129.0
$SiCl_4 + H_2O = SiCl_2O + 2HCl$	245.3	224.1	226.7	180.9

Gibbs free energ,y which is consistent with the negative energy of Si−Cl bond hydrolysis.

Although the absolute values of thermodynamic functions obtained at the G2(MP2) and DFT levels of theory are rather different, all of the trends represented by the two methods are the same. It should also be noted that DFT gives reaction energies and thermal effects that are higher in absolute values than the corresponding results from the extrapolation method. Thus, we can consider the DFT results as a reliable upper bound of the reaction energy that can be used for obtaining qualitative results for processes involving larger molecules.

Table 5 summarizes the energies for all the reactions involved in the hydrolysis reaction mechanism for $SiCl_4$. The reaction mechanism consists of the reactions of primary hydrolysis, condensation (both hetero- and homofunctional condensation), as well as the reactions of linear polymerization, formation of cyclic polymers and the formation of dichlorosilanone $Cl_2Si{=}O$ and silicic acid $(HO)_2Si{=}O$. The two last reactions are important because they are discussed sometimes as intermediates in the gas-phase hydrolysis of $SiCl_4$.

The results presented in Table 5 show that both the enthalpies and Gibbs free energies of the reactions forming $Cl_2Si{=}O$ and $(HO)_2Si{=}O$ have very high positive values, which makes the formation of these compounds highly improbable under equilibrium conditions. One can conclude that the concentration of $Cl_2Si{=}O$ in an equilibrium mixture is neglibly low and that the observation of this species in mass spectrometry experiments is a consequence of secondary nonequilibrium processes, probably occurring inside the ionization chamber of the instrument. The same conclusion can be reached for silicic acid, which is also a very high energy molecule with quite low concentrations in a gas-phase mixture under equilibrium conditions.

As is evident from Table 5, both the primary hydrolysis reactions and the condensation reactions are thermodynamically favorable, exothermic processes at all stages of hydrolysis. Because the Si−Cl bond hydrolysis is exothermic, the more

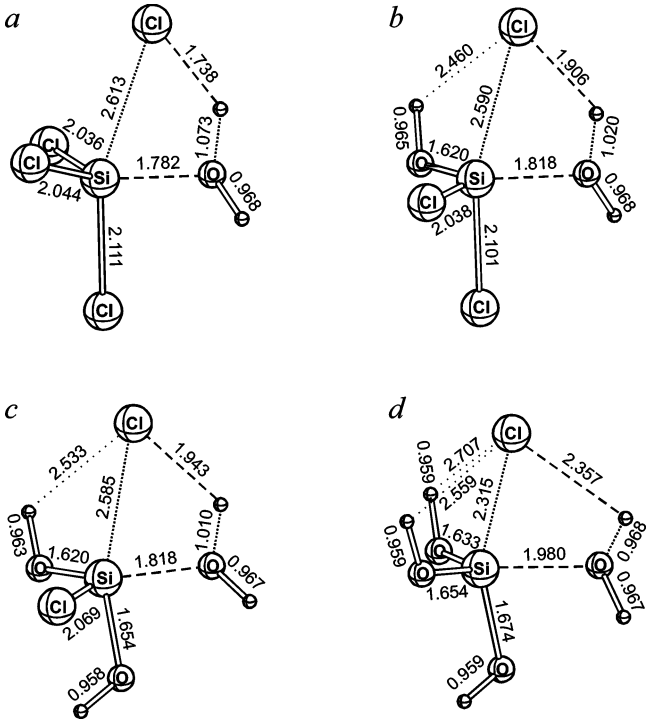

Figure 1. B3LYP/6-311++G(2d,2p) optimized structures of transition states: (a) TS1a; (b) TS1b; (c) TS1c; (d) TS1d. Hereafter, the dashed line marks a forming bond, the dotted line a breaking bond, and sparse dashed line an additional hydrogen bond.

extensively the hydrolysis occurs the more energy is evolved in the reaction. Because the values of the reaction enthalpy and Gibbs free energy are quite high, the equilibrium should be shifted completely to the side of products. Thus, there are no thermodynamic restrictions on the hydrolysis of $SiCl_4$ and this reaction should be controlled by kinetic factors only. As mentioned above, this is a fundamental difference between the hydrolysis of $SiCl_4$ and the analogous process for SiF_4.

It is interesting that the cyclic polymer structures $[-SiCl_2-O-]_n$ formed in the hydrolysis are thermodynamically profitable for $n = 3$ and are more profitable than the linear polymers, in contrast with SiF_4 cyclization where the cyclic polymers prevail over the linear polymers only above $n = 6$ or 7. This can lead to a larger proportion of cyclic structures in SiO_2 formed by the hydrolysis of $SiCl_4$ and to a larger proportion of small cyclic polymers in products than occurs during the hydrolysis of SiF_4. Clearly, this can have an effect on the physical properties of the formed materials.

Kinetics of Bimolecular Reactions. Consistent with the reaction scheme (1)−(3), it is expected that the primary hydrolysis step and the condensation step are regular bimolecular reactions with four-membered cyclic transition states, as is well-documented for many similar systems. Figure 1a shows the structure located for the transition state of the primary hydrolysis reaction, whereas Figure 1b−d show the structures of the transition state for the three additional hydrolysis steps. The corresponding energies and the thermodynamic parameters of the transition states are listed in Table 6. As can be seen, the activation energy for the first Si−Cl bond hydrolysis reaction is 107 kJ/mol and decreases in the sequence:

$$SiCl_4 > SiCl_3OH > SiCl_2(OH)_2 > SiCl(OH)_3$$

Similarly, the condensation steps in the hydrolysis of $SiCl_4$ as given in reactions 1−3 can be considered as bimolecular reactions with transition states shown in Figures 2 and 3. Table 7 lists the calculated energies and the kinetic parameters of the corresponding structures. One can conclude from a comparison of the data presented in Tables 6 and 7 that the condensation steps have higher activation barriers and are the rate-limiting steps of the process. The homofunctional condensation (4a) is more favorable than the heterofunctional condensation (4b) from the point of view of activation energy. Thus, it clearly prevails under conditions where water is abundant. However, when there is a shortage of water in a mixture, the heterofunctional reaction may dominate, which can change the apparent activation energy.

The conclusion that the condensation step is the rate-limiting step of the overall process is in agreement with experimental observations[8] on the existence of OH-containing species in a mixture of partially hydrolyzed $SiCl_4$, and the slow disappearance of these species at higher temperature. It is also interesting that the most kinetically favorable step among the $SiCl_{4-x}(OH)_x$ condensation reactions is an intermediate step with $x = 3$, not 4 as might be expected from a comparison with the results of the primary hydrolysis reactions (Table 7).

The most important conclusion from the calculated results is that no bimolecular reactions can describe correctly the observed experimental features found for the low-temperature hydrolysis. First, the activation energy of the rate-limiting step is too high (107 kJ/mol) to permit rapid hydrolysis at 20−50 °C. The corresponding rate constant calculated by the conventional transition state theory equation

$$k = \frac{k_B T}{h} \frac{Q_{TS}}{\prod_i Q_{Ri}} e^{-\Delta H_0/RT} \left(\frac{p_0}{RT}\right)^{-\Delta \nu^{\ddagger}} \qquad (5)$$

(Q_{TS} and Q_{Ri} are the partition functions of the transition state and the reagent i, respectively, $\Delta H_0 = E_a + \mathrm{ZPE}$, p_0 is the standard pressure, and $\Delta \nu^{\ddagger}$ is the change in the number of molecules due to transition state formation) has an extremely low value, $\sim 10^{-9}$ $cm^3 \cdot mol^{-1} \cdot s^{-1}$.

Second, the bimolecular reactions considered here cannot be combined in any manner to yield the second-order dependence on water measured in the low-temperature hydrolysis reaction.[9,10] Finally, these simple bimolecular reactions with highly positive activation energies cannot explain the negative value of apparent activation energy observed in the temperature range 20−100 °C.[10]

Multimolecular Reaction Kinetics. The failure of bimolecular kinetics to describe the experimental features observed in the low-temperature hydrolysis stimulated the search for an alternative reaction mechanism. One possibility is to consider complexes between the various molecules present in the reaction mixture, and primarily with water. The idea of describing the low-temperature hydrolysis via the formation of complexes between water and reaction intermediates was suggested previously in ref 9 where a reaction scheme involving a reaction between the $SiCl_4 \cdot H_2O$ complex and a water dimer $(H_2O)_2$ was proposed. However, the scheme was neither proved by kinetics experiments nor by any theoretical calculation. No additional attention was paid to the structure or estimate of energies for the proposed intermediates. Moreover, the scheme suggested in ref 9 was based on the assumption of fast condensation steps, which is not consistent with the more accurate experiments.[10]

In this work, we tried to locate the structures of the transition states of the hydrolysis reactions that occur with the participation of two and three molecules of water. For the reaction with two water molecules, two different transition states were located. The structure of the first, TS4a, is open with water molecules

TABLE 6: Calculated Energies and Thermodynamic Parameters of Transition States for the Bimolecular Elementary Reactions of Primary Hydrolysis Calculated at the B3LYP/6-311++G(2d,2p) Level

elementary reaction	geometry of transition state	ν_{im},[a] kJ/mol	$E_{tot}^{\ddagger}$, au	$\Delta E^{\ddagger}$,[b] kJ/mol	$\Delta(E^{\ddagger}+ZPE)$,[c] kJ/mol	$\Delta H^{\ddagger}$, kJ/mol	$\Delta G^{\ddagger}$, kJ/mol
$SiCl_4 + H_2O \rightarrow SiCl_3OH + HCl$	TS1a, Figure 1a	302i	−2207.0526212	105.0	107.0	101.1	142.5
$SiCl_3OH + H_2O \rightarrow SiCl_2(OH)_2 + HCl$	TS1b, Figure 1b	182i	−1822.6956728	76.0	85.8	78.6	129.5
$SiCl_2(OH)_2 + H_2O \rightarrow SiCl(OH)_3 + HCl$	TS1c, Figure 1c	174i	−1438.3285975	74.1	85.1	78.0	127.5
$SiCl(OH)_3 + H_2O \rightarrow Si(OH)_4 + HCl$	TS1d, Figure 1d	87i	−1053.9669023	55.5	71.1	63.4	115.6

[a] Imaginary frequency, cm^{-1}. [b] Activation energy. [c] Activation energy including the ZPE.

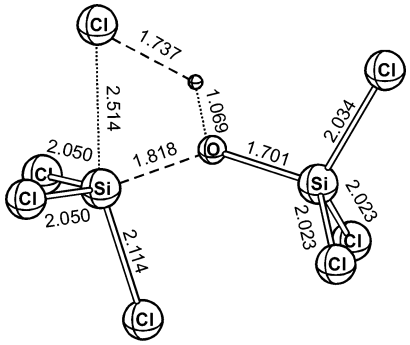

Figure 2. B3LYP/6-311++G(2d,2p) optimized structure of the transition state TS2.

coordinated each to another in a manner similar to that of the water dimer (Figure 4a). The second, TS4b, is a cyclic transition state with two water molecules forming a four-membered ring (Figure 4b).

Table 8 presents the energetic values and the kinetic parameters of the corresponding termolecular hydrolysis reaction of $SiCl_4$:

$$SiCl_4 + 2H_2O \rightarrow [TS4] \rightarrow SiCl_3OH + H_2O + HCl \quad (6)$$

As evident from the table, the coordination of a second water molecule to the transition state of the regular bimolecular reaction results in a decrease in the activation energy of the Si−Cl bond hydrolysis reaction by 50 kJ/mol. It is interesting that the energy of dimerization for water itself (experimental value 22.6 ± 2.9 kJ/mol,[28] BSSE-corrected B3LYP/6-311++G(2d,2p) value 19.1 kJ/mol) cannot explain such a large decrease in the activation energy. The coordination of the second water molecule results in an increases in the entropy of the system and consequently the Gibbs free energy of activation. Thus, the effect of the coordination of a second water molecule to $\Delta G^{\ddagger}$ is only about 15−20 kJ/mol for both TS4a and TS4b. The main effect of water coordination is a change in the acidity of the H atom coordinated to the silicon and a weakening of the "breaking" O−H bond. Nevertheless, the activation energy of the termolecular reaction 6 still remains too high to explain the fast hydrolysis reaction at room temperature.

Another alternative to bimolecular kinetics is the reaction described formally by

$$SiCl_4 + 3H_2O \rightarrow [TS5] \rightarrow SiCl_3OH + HCl + 2H_2O \quad (7)$$

occurring through a four-molecule transition state TS5. Similar to TS4, two different conformations were located for the transition state TS5. They are shown as TS5a and TS5b in Figure 5. The calculated activation parameters of reaction 7 are presented in Table 8. As shown in the table, the activation energy of this reaction calculated relative to the uncoordinated reactants is negative. Of the two conformations, the closed structure of transition state TS5b with an ice-like configuration of water molecules is more profitable from an energetic point of view. The formation of this kind of structure decreases the Gibbs free energy of activation by about 30 kJ/mol. Because the rate constants are strongly influenced by the height of the activation barrier, we tried to obtain a more accurate value of ΔH_0 using the G2(MP2) energy calculated for the structure and frequencies of the transition state obtained at the B3LYP/6-311++G(2d,2p) level. The results of the G2(MP2)//B3LYP/6-311++G(2d,2p) calculation are also listed in Table 8 (values in brackets). The G2(MP2) calculations reduce the barrier height, keeping, however, the relative order of the rate constants for reactions (1a), (6), and (7) the same as for DFT results.

Figure 6 shows the temperature dependence of the reaction rate constants for the bimolecular Si−Cl bond hydrolysis reaction (transition state TS1), the corresponding termolecular reaction 6 (transition states TS4a and TS4b), and reaction 7 proceeding through transition states TS5a and TS5b at the B3LYP/6-311++G(2d,2p) level. As shown on the diagram, in the low-temperature region (up to 800 K) the rate constant for the bimolecular hydrolysis reaction 1a has a negligibly small value whereas reactions 6 and 7 have significantly higher values. The formation of a four-molecule transition state results in significant changes to the temperature dependence of the reaction rate: the rate constant for reaction 7 decreases with increasing temperature in the range 300−350 K (i.e., a negative value of the apparent activation energy). The reason for the decrease in the rate of reaction 7 is a slow temperature dependence of the exponential factor of rate constant k_7. Because the ΔH_0 value in this reaction is small, the temperature dependence of the exponential factor is very weak and the temperature dependence of the rate constant is mainly influenced by the preexponential factor, namely, by the partition functions ratio $Q_{TS}/(Q_{SiF_4}Q_{H_2O}{}^3)$.

Because the rate-limiting step of the hydrolysis reaction is condensation, it is interesting to discuss what is an apparent activation energy for the low-temperature hydrolysis estimated in refs 9 and 10 and measured in the high-temperature region.[10] The measurements were conducted in an enclosed volume under isochoric conditions. Changes in $SiCl_4$ concentrations were estimated by observing a decrease in the infrared intensity of the vibrational band of $SiCl_4$ at 608 cm^{-1}. Without considering possible changes in the spectral band intensity due to coordination, pressure changes, and other small effects, one can conclude that, under these conditions, the observed changes in intensity correspond to a decrease in $SiCl_4$ concentration. Thus, the measured initial rate constant is the rate constant for the first step of hydrolysis, i.e., reaction 1a. This explains why we observe the kinetic features of the reaction of $SiCl_4$ instead of apparent kinetic parameters of the overall hydrolysis, which is controlled by the rate-limiting condensation reaction. In addition, polymolecular reactions can take place not only for the first Si−Cl bond hydrolysis and then condensation of $SiCl_3OH$, but also for further steps (successive Si−Cl bond hydrolysis and condensation for $SiCl_{4-x}(OH)_x$).

Comparison with Experimental Data. Figure 7 shows the initial rates of $SiCl_4$ hydrolysis calculated on the basis of

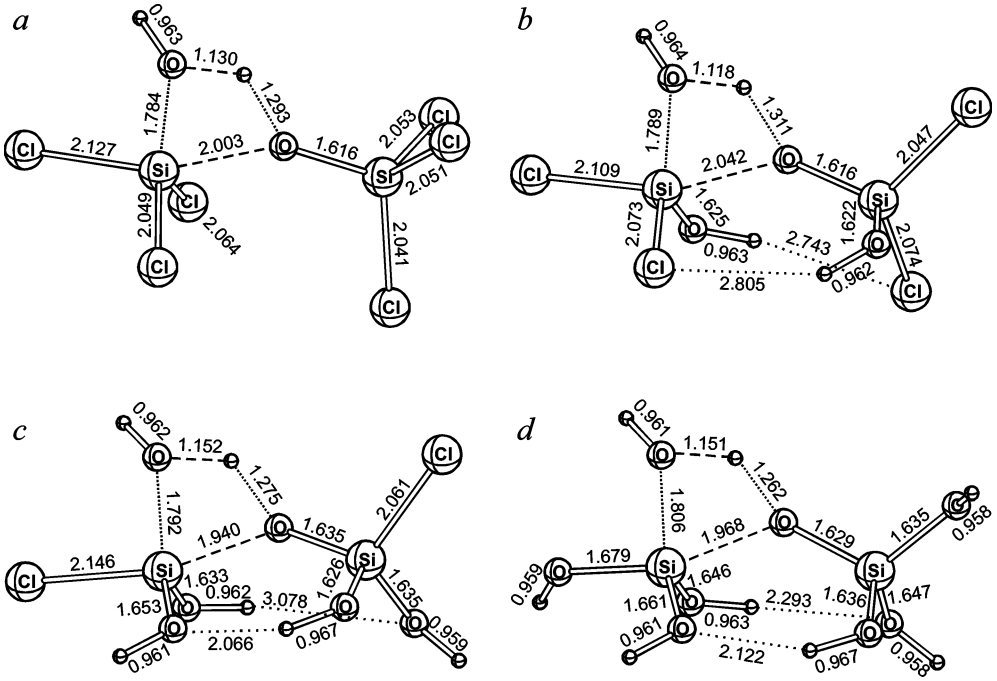

Figure 3. B3LYP/6-311++G(2d,2p) optimized structures of transition states: (a) TS3a; (b) TS3b; (c) TS3c; (d) TS3d.

TABLE 7: Calculated Energies and the Thermodynamic Parameters of Transition States for the Bimolecular Elementary Reactions of the Condensation Steps of $SiCl_4$ Hydrolysis (B3LYP/6-311++G(2d,2p))

elementary reaction	geometry of transition state	ν_{im},[a] kJ/mol	$E_{tot}^{\ddagger}$, au	$\Delta E^{\ddagger}$,[b] kJ/mol	$\Delta(E^{\ddagger}+ZPE)$,[c] kJ/mol	$\Delta H^{\ddagger}$, kJ/mol	$\Delta G^{\ddagger}$, kJ/mol
$SiCl_3OH + SiCl_4 \rightarrow SiCl_3-O-SiCl_3 + HCl$	TS2, Figure 2	217*i*	−3876.8397355	140.3	137.1	135.8	184.2
$2SiCl_3OH \rightarrow SiCl_3-O-SiCl_3 + H_2O$	TS3a, Figure 3a	993*i*	−3492.4758888	129.4	126.2	124.6	177.7
$2SiCl_2(OH)_2 \rightarrow SiCl_2(OH)-O-SiCl_2(OH) + H_2O$	TS3b, Figure 3b	880*i*	−2723.7476776	110.3	108.7	106.2	160.4
$2SiCl(OH)_3 \rightarrow SiCl(OH)_2-O-SiCl(OH)_2 + H_2O$	TS3c, Figure 3c	1099*i*	−1955.0196064	85.1	87.1	82.8	140.8
$2Si(OH)_4 \rightarrow Si(OH)_3-O-Si(OH)_3 + H_2O$	TS3d, Figure 3d	1044*i*	−1186.2781676	93.0	95.1	90.9	148.7

[a] Imaginary frequency, cm^{-1}. [b] Activation energy. [c] Activation energy including the ZPE.

TABLE 8: B3LYP/6-311++G(2d,2p) and G2(MP2)//B3LYP/6-311++G(2d,2p) (in Square Brackets) Calculated Energies and Thermodynamic Parameters of Transition States for the Primary Hydrolysis Reactions of $SiCl_4$

geometry of transition state	ν_{im},[a] kJ/mol	$E_{tot}^{\ddagger}$, au	$\Delta E^{\ddagger}$,[b] kJ/mol	$\Delta(E^{\ddagger}+ZPE)$,[c] kJ/mol	$\Delta H^{\ddagger}$, kJ/mol	$\Delta G^{\ddagger}$, kJ/mol
		Reaction $SiCl_4 + H_2O \rightarrow SiCl_3OH + HCl$				
TS1a, Figure 1*a*	302i	−2207.0526212	105.0 [103.4]	107.0 [105.4]	101.1 [99.6]	142.5 [140.9]
		Reaction $SiCl_4 + 2\ H_2O \rightarrow SiCl_3OH + HCl + H_2O$				
TS4a (open), Figure 4a	256i	−2283.5369230	46.5	57.7	49.7	127.7
TS4b(cyclic), Figure 4b	226i	−2283.5407040	36.6 [30.3]	49.9 [43.1]	39.1 [32.8]	121.3 [114.9]
		Reaction $SiCl_4 + 3\ H_2O \rightarrow SiCl_3OH + HCl + 2\ H_2O$				
TS5a(open), Figure 5c	253i	−2360.0193902	−7.1[d]	13.6	1.2	122.3
TS5b(closed), Figure 5d	108i	−2360.0261989	−25.0[d] [−35.3][d]	0.5 [−9.8][d]	−11.9[d] [−22.2]	111.5 [101.2]

[a] Imaginary frequency, cm^{-1}. [b] Activation energy. [c] Activation energy including the ZPE. [d] The negative E_a values are calculated relative to the isolated (uncoordinated) reactants.

theoretical rate constants (calculated at G2(MP2) level) in comparison with experimental rates from ref 9 and 10. In Figure 7a the reaction rates corresponding to the high-temperature hydrolysis are shown. Two series of experimental values were recalculated from Figures 2 and 4 of ref 10; the theoretical values correspond to the experimental partial pressures of reagents $p_0[SiCl_4] = 1.01$ kPa, $p_0[H_2O] = 2.03$ kPa. Comparison between the experimental and theoretical initial rates demonstrates very good agreement, and, consequently, confirms the proposal that the hydrolysis in the high-temperature region is described by the bimolecular reaction 1 occurring through the transition state TS1.

In contrast with the high-temperature hydrolysis reaction, comparison between the calculated and experimental data under low-temperature conditions shows large discrepancies. Figure 7b shows the experimental initial rates taken from ref 9 and 10 and the corresponding values for the reactions occurring through transition states TS4b and TS5b. All of the values were calculated at concentrations corresponding to the conditions of ref 10. As follows from the figure, the termolecular reaction 6 leads to a positive apparent activation energy, whereas reaction 7 is characterized by a negative value of the apparent E_a, which is consistent with the experimental trend. However, the absolute values of the theoretical rates are quite far from the experimental ones and are characterized by significantly lower values. As a rule, the calculated values are lower by 6−7 orders of magnitude from the experimental ones. Such a large discrepancy between the experimental and theoretical values cannot be explained by

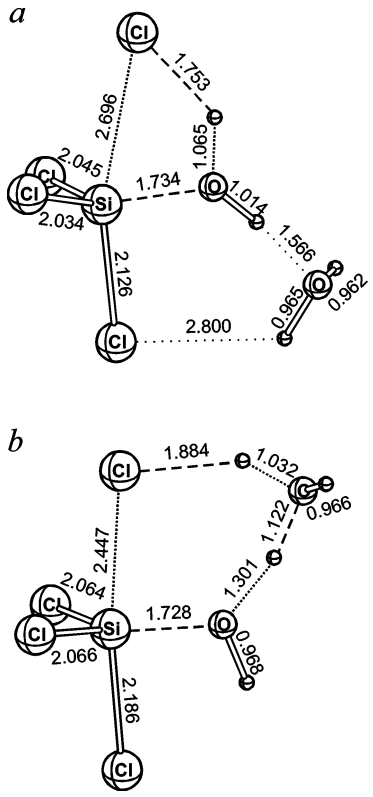

Figure 4. B3LYP/6-311++G(2d,2p) optimized structures of transition states: (a) TS4a; (b) TS4b.

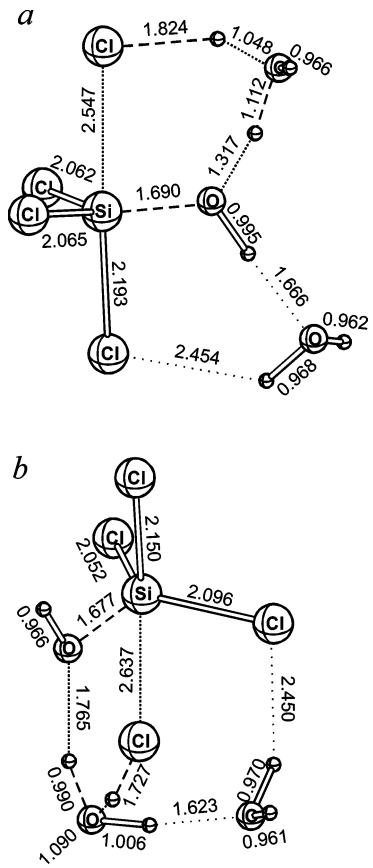

Figure 5. B3LYP/6-311++G(2d,2p) optimized structures of transition states: (a) TS5a; (b) TS5b.

the deficiencies of the quantum chemical method or by errors arising from the modest accuracy of the thermodynamic or kinetic models. Rather, the large discrepancy between the

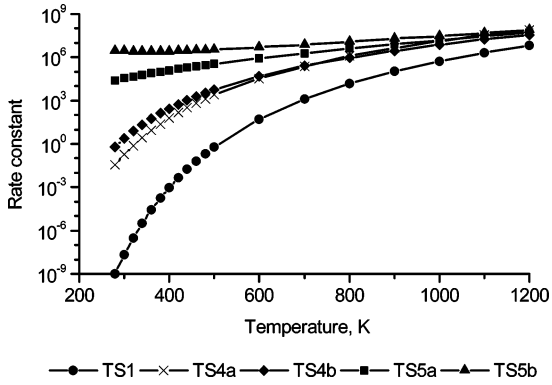

Figure 6. Calculated rate constants for $SiCl_4$ hydrolysis occurring through the different transition states (B3LYP/6-311++G(2d,2p) results). The units are $(mol^{-1}\cdot cm^3)^n\cdot s^{-1}$, where $n = 1-3$ for the transition states TS1, TS4, and TS5, correspondingly.

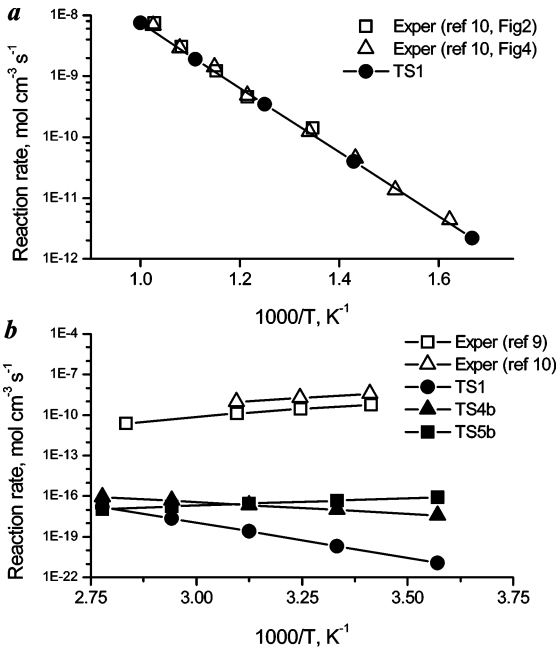

Figure 7. Comparison between the experimental and calculated initial rates of the gas-phase hydrolysis of $SiCl_4$ at different temperatures: (a) high-temperature hydrolysis (600−1000 K); (b) low-temperature hydrolysis (270−360 K).

experimental and calculated results leads us to conclude that the low-temperature hydrolysis of $SiCl_4$ cannot be explained by reactions 6 or 7 occurring in the gas phase. Thus, the suggestion that the gas-phase hydrolysis of $SiCl_4$ is accelerated by coordination of additional water molecules to the transition structure is not supported by the experimental data, and other explanations should be offered to describe the anomalous kinetics of the gas-phase hydrolysis under low-temperature conditions.

In addition to the purely molecular processes considered here, other processes may be proposed to explain the observed features of the $SiCl_4$ hydrolysis reaction at low temperatures: (i) radical formation and further radical-chain reactions, (ii) reactions occurring on small water droplets that probably form in the reaction volume, and (iii) heterophase reactions on the walls of the equipment. However, the first alternative is not consistent with the decrease of the reaction rate with an increase of temperature. With respect to the second alternative, it is hard to envision that the effect of liquid-phase reactions will be significant under the experimental conditions described above (the water pressure is 2−10 times lower than the dew point at

a given temperature). Heterophase reactions occurring at the walls covered by layers of adsorbed water seems to be the most likely explanation. Because the isotherm for water adsorption at pressures close to the saturation pressure can show an order larger than 1, it can probably explain the second-order dependence for water observed experimentally. Indeed, it can also explain the negative activation energy because increasing temperature results in significant desorption of water from the surface. However, because direct measurements of the surface hydrolysis reaction are not available, the mechanism of the low-temperature hydrolysis remains uncertain and requires further investigation.

Conclusions

On the basis of quantum chemical modeling, one can conclude that the hydrolysis of a Si−Cl bond in $SiCl_4$ is an exothermic and thermodynamically favorable process, in contrast to the analogous reaction of SiF_4. This process has no thermodynamic restrictions and is controlled by kinetic factors only.

The calculations predict that an equilibrium mixture of partially hydrolyzed $SiCl_4$ will contain a large amount of hydroxyderivatives $SiCl_{4-x}(OH)_x$. Among them, species with lesser x are thermodynamically favored, which is supported by the available experimental data. Also, the concentrations of $Cl_2Si{=}O$ and $(HO)_2Si{=}O$ in the equilibrium gas-phase hydrolytic mixture will be negligibly small because of high Gibbs free energies of these structures.

For the overall hydrolysis process, the rate-limiting step is an elementary reaction involving $SiCl_3OH$ condensation and resulting in siloxane formation. From the kinetic point of view, the homofunctional condensation reaction 4a is more favorable than the hetero-functional one (4b).

A bimolecular mechanism for the hydrolysis of Si−Cl bonds and $SiCl_3OH$ condensation is in good agreement with the experimentally determined reaction order, temperature dependence of the rate constant, and absolute values of the initial reaction rate in the gas-phase hydrolysis of $SiCl_4$ at high temperatures (600−1000 K). However, the experimentally observed reaction rate values of hydrolysis in the low-temperature region (300−400 K) cannot be described by bimolecular kinetics. The proposal about coordination of one or two additional water molecules is inconsistent with the experimental results. Although reaction 7 demonstrates the proper sign of the apparent activation energy, the calculated initial rates for the reactions occurring through two- and three-molecular transition states are significantly lower than the observed ones. Thus, the actual mechanism of the low-temperature hydrolysis of $SiCl_4$ in the gas phase under the above conditions requires further investigation.

Acknowledgment. This work was supported by the Russian Foundation for Basic Research (Project No. 00-03-32094, 03-03-33120). S.I. and P.G. thank the Alfred Wegener Institute for Polar and Marine research for the fellowship support. We also express our gratitude to one of the anonymous referees for his valuable comments.

References and Notes

(1) Bagatur'yants, A. A.; Alfimov, M. V.; Ignatov, S. K.; Razuvaev, A. G.; Gropen, O. *Mater. Sci. Semicond. Proc.* **2000**, *3*, 71.

(2) Devyatykh, G. G.; Bulanov, A. D.; Gusev, A. V.; Sennikov, P. G.; Prokhorov, A. M.; Dianov, E. M.; Pohl, H.-J. *Dokl. Chem.* **2001**, *376*, 492 (Engl. Transl.).

(3) Furman, A. A. *Inorganic chlorides*; Chemistry: Moscow, 1980; p 183.

(4) Bazant, V.; Chvalovsky, V.; Rathovsky, J. *Organosilicon compounds*; Academic Press: New York, 1965; Vol. 1, p 41.

(5) *The chemistry of organic Silicon compounds*; Patai, S., Rappoport, Z., Eds.; John Wiley and Sons Ltd.: New York, 1989.

(6) Voronkov, M. G.; Mileshkevich, V. P.; Yuzhelevsky, Y. A. *The Siloxane Bond*; Consultants Bureau: New York, 1978.

(7) Shumb, W. C.; Stevens, A. J. *J. Phys. Chem.* **1950**, *72*, 3178.

(8) Kometani, T. Y.; Darwin, L. W.; Luongo, J. P. *Anal. Chem.* **1987**, *59*, 1089.

(9) Sagitova, V. G.; Chernyak, V. I. *Zhurn. Obsh. Khimii* **1983**, *53* (2), 397.

(10) Kochubei, V. F. *Kinet. Katal.* **1997**, *38* (2), 234.

(11) Kudo, T.; Gordon, M. S. *J. Am. Chem. Soc.* **1998**, *120*, 11432.

(12) Kudo, T.; Gordon, M. S. *J. Phys. Chem. A* **2000**, *104*, 4058.

(13) Okumoto, S.; Fujita, N.; Yamabe, S. *J. Phys. Chem. A* **1998**, *102*, 3991.

(14) Ignatyev, I. S.; Partal, F.; López González, J. J. *Chem. Phys. Lett.* **2003**, *368*, 616.

(15) Jug, K.; Gloriozov, I. P. *Phys. Chem. Chem. Phys.* **2002**, *4*, 1062.

(16) Jug, K.; Gloriozov, I. P. *J. Phys. Chem. A* **2002**, *106*, 4736.

(17) Kumar, A.; Homann, T.; Jug, K. *J. Phys. Chem. A* **2002**, *106*.

(18) Frisch, M. J.; Trucks, G. W.; Schlegel, H. B.; Scuseria, G. E.; Robb, M. A.; Cheeseman, J. R.; Zakrzewski, V. G.; Montgomery, J. A., Jr.; Stratmann, R. E.; Burant, J. C.; Dapprich, S.; Millam, J. M.; Daniels, A. D.; Kudin, K. N.; Strain, M. C.; Farkas, O.; Tomasi, J.; Barone, V.; Cossi, M.; Cammi, R.; Mennucci, B.; Pomelli, C.; Adamo, C.; Clifford, S.; Ochterski, J.; Petersson, G. A.; Ayala, P. Y.; Cui, Q.; Morokuma, K.; Malick, D. K.; Rabuck, A. D.; Raghavachari, K.; Foresman, J. B.; Cioslowski, J.; Ortiz, J. V.; Stefanov, B. B.; Liu, G.; Liashenko, A.; Piskorz, P.; Komaromi, I.; Gomperts, R.; Martin, R. L.; Fox, D. J.; Keith, T.; Al-Laham, M. A.; Peng, C. Y.; Nanayakkara, A.; Gonzalez, C.; Challacombe, M.; Gill, P. M. W.; Johnson, B. G.; Chen, W.; Wong, M. W.; Andres, J. L.; Head-Gordon, M.; Replogle, E. S.; Pople, J. A. *Gaussian 98*, revision A.3; Gaussian, Inc.: Pittsburgh, PA, 1998.

(19) Schmidt, M. W.; Baldridge, K. K.; Boatz, J. A.; Elbert, S. T.; Gordon, M. S.; Jensen, J. H.; Koseki, S.; Matsunaga, N.; Nguyen, K. A.; Su, S. J.; Windus, T. L.; Dupuis, M.; Montgomery, J. A. *J. Comput. Chem.* **1993**, *14*, 1347.; Granovsky, A. A. *PC GAMESS* home page: http://classic.chem.msu.su/gran /gamess/index.html.

(20) Curtiss, L. A.; Raghavachari, K.; Pople, J. A. *J. Chem. Phys.* **1993**, *98*, 1293.

(21) Jiménez-Vázquez, H. A.; Tamariz, J.; Cross, R. J. *J. Phys. Chem. A* **2001**, *105*, 1315.

(22) East, A. L. L.; Radom, L. *J. Chem. Phys.* **1997**, *106*, 6655.

(23) Pitzer, K. S.; Gwinn, W. D. *J. Chem. Phys.* **1942**, *10*, 428. Pitzer, K. S. *J. Chem. Phys.* **1946**, *14*, 239.

(24) Ignatov, S. K.; Razuvaev, A. G.; Sennikov, P. G.; Nabviev, Sh. Sh. *Proceedings of the VIIIth Joint International Symposium "Atmospheric and ocean optics. Atmospheric physics"*, June 25−29, 2001, Irkutsk; 2001; p 93.

(25) Ignatov, S. K.; Sennikov, A. G.; Razuvaev, A. G.; Chuprov L. A. *Russ. Chem. Bull.* **2003**, 4, 837.

(26) Wichmann, D. Ph.D. Thesis, Universität Hannover, 1997, p 77.

(27) Su, M.-D.; Schlegel, H. B. *J. Phys. Chem.* **1993**, *97*, 9981.

(28) Halkier, A.; Koch, H.; Jørgensen, P.; Christiansen, O.; Beck Nielsen, I. M.; Helgaker, T. *Theor. Chem. Acc.* **1997**, *97*, 150.